Effect of Sintering Temperature on Micro Structural and Impedance Spectroscopic Properties of $Ni_{0.5}Zn_{0.5}Fe_2O_4$nano Ferrite

Davuluri Venkatesh[1] , K V Ramesh[1*] and C V S S Sastry[2]

[1]*Center for Materials Research, Department of Physics, GITAM Institute of Science, GITAM University, Rushikonda, Visakhapatnam, Andhra Pradesh-530045, India*
[2] *Government Degree College, Chodavaram, Visakhapatnam, Andhra Pradesh, India*

[*]Corresponding author: *kvramesh11@gmail.com*

Abstract. Ni-Zn nanoferrite $Ni_{0.5}Zn_{0.5}Fe_2O_4$ is prepared by citrate gel auto combustion method and sintered at various temperatures 800, 900, 1000, 1100 and 1200^0C. The room temperature x-ray diffraction conforms that the single phase spinel structure is formed. Crystallite size and density were increased with increasing of sintering temperature. From Raman spectroscopy all sintered samples are single phase with cubic spinel structure belong to Fd3m space group. From surface morphology studies it is clearly observed that the particle size increased with increasing of sintering temperature. Impedance spectroscopy revel that increasing of conductivity is due to grain resistance is decreased with increasing of sintering temperature. Cole-Cole plots are studied from impedance data. The electrical modulus analysis shows that non-Debye nature of $Ni_{0.5}Zn_{0.5}Fe_2O_4$ ferrite.

Keywords: Ni-Zn ferrite, Auto combustion, Impedance spectroscopy.

INTRODUCTION

The spinel structured nano crystalline Ni-Zn ferrite having chemical formula $Ni_{0.5}Zn_{0.5}Fe_2O_4$ is most versatile magnetic material for electronic devices, inductors, magnetic media, and high frequency applications. Due to their high resistivity, saturation magnetization, low eddy current losses and high Curie temperature [1-3]. The spinel structured Ni-Zn ferrites have both tetrahedral (A) and Octahedral (B) Sites with Molecular formula $[Fe^{3+}\ Zn^{2+}]^A\ [Ni^{2+}\ Fe^{3+}]^B\ O_4$ Where Zn^{2+} ions prefer to occupy tetrahedral (A) site, Ni^{2+} ions prefer to occupy octahedral (B) site and Fe^{3+} ions occupy both A and B sites. The cation distribution of A and B site depends on the method of preparation, stoichiometric composition, concentration of impurity and ionic radii [4-5]. There are different methods for preparation of Ni-Zn ferrites. Such as Solid state reaction [6], high energy ball milling [7], co-precipitation method [8], hydrothermal synthesis [9], sol gel method [10], citrate gel auto combustion method [11].

$Ni_{0.5}Zn_{0.5}Fe_2O_4$ is well established in conventional ceramic method but it needs high calcination temperature. Applying of high temperatures for long time some constituent elements like zinc volatilization may take place. This may results to formation of Fe^{2+} ions, which may cause to increase of electron hoping mechanism and decreasing of resistivity [12] and also this type of preparation techniques have homogeneity of particles is very less. Synthesis of nano particle in auto combustion methods, no need of high temperature and most of the particles are formed in uniform size. Preparing of nano ferrites in below 200^0C temperature Citrate gel auto combustion method is promising. In our previous report [13] we reported that cation distribution, microstrain and magnetic properties of $Ni_{0.5}Zn_{0.5}Fe_2O_4$ ferrite sintered at various sintering temperatures. In this present communication our

interest is to study effect of grain size on Structural, electrical and Impedance spectroscopic properties of $Ni_{0.5}Zn_{0.5}Fe_2O_4$ system synthesized via citrate gel auto combustion method and sintered at different sintering temperatures (800, 900, 1000, 1100, 1200^0C).

EXPERIMENTAL

The nano $Ni_{0.5}Zn_{0.5}Fe_2O_4$ferrite system was prepared by citrate gel auto combustion method. In this method all high purity chemicals such as Nickel nitrate, (Ni $(NO_3)_2.6H_2O$), Zinc nitrate (Zn $(NO_3)_2.6\ H_2O$), Ferric nitrate (Fe $(NO_3)_2.9\ H_2O$), and Citric acid ($C_6H_8O_7$) were used. All nitrates were weighed accordingly and dissolved in double distilled deionized water as per stoichiometry. The raw nitrate solution mixture was kept on a magnetic stirrer with hot plate and applies continuous stirring to get homogeneity. Temperature was maintained at 65ºC for few minutes after that the chelating agent citric acid was mixed into the nitrate solution. Now by increase the temperature viscous gel was formed and it finally becomes powder. The obtained powder was mixed with binder polyvinyl alcohol and pressed into pellets 10mm diameter and 3mm thickness by applying pressure of 5 tons/inch^2. The samples were sintered at 800ºC, 900ºC, 1000ºC, 1100ºC, and 1200ºC in air for 4 hours. In sintering process the oxide layer is formed to reduce this oxide layer the pellets were polished. For electrical contact silver paste was applied on both sides of pellets and heated at200^0C for one hour.

The room temperature powder X-ray diffraction data was carried out by using of Pan-Analytical X'pertPRO diffraction meter with CuKα (=1.5406 A^0).The crystal structure, crystallite size are estimated from standard relations. The room temperature Raman data of all sintered samples made on by using of Horiba Scientific Lab Ram HR Raman spectrometer with excitation wavelength of 532 nm. The surface morphology studies of all sintered pellets were performed on ZEISS Scanning electron micro scope with accelerating voltage 10 kV. And also impedance data of all sintered samples were performed on PSM-1735 Newton 4thLtd. In frequency range (1 Hz to 10 MHz).

RESULTS AND DISCUSSIONS

The X-ray diffractrograms of $Ni_{0.5}Zn_{0.5}Fe_2O_4$ ferrite sintered at various temperatures such as 800ºC, 900ºC, 1000ºC, 1100ºC, and 1200ºC were shown in figure 1. From figure1 which is indicating that all samples exhibiting single phase spinel cubic structure. The experimental lattice parameter was calculated by using of standard relation [13].

$$a_{exp} = d_{hkl}\sqrt{(h^2 + k^2 + l^2)}$$

Where a_{exp} is experimental lattice parameter, d_{hkl} is interplanar spacing.

The crystallite size of most intense peak (311) of $Ni_{0.5}Zn_{0.5}Fe_2O_4$ ferrite was calculated by using the Debye-Scherer relation [13] as given below.

$$D_{311} = \frac{0.9\lambda}{\beta\,Cos\theta}$$

Where λ is wavelength, β is full width at half maximum (FWHM) and is θ angle of diffraction. The crystallite sizes of all sintered samples were increased with increasing of sintering temperature and the density of samples is also increased with increasing of sintering temperature. The obtained crystallite size, lattice parameter and density of the sample sintered at different temperatures are reported in table 1.

Raman spectroscopy is used to study the vibrational spectra of spinel ferrite materials. The cubic spinel $Ni_{0.5}Zn_{0.5}Fe_2O_4$ nanoferrite belongs to *Fd3m* space group with eight formula ($8M^{II}Fe_2^{III}O_4$) units per unit cell. The unit cell containing 56 atoms and the smallest Braves cell consists of 14 atoms. Therefore 42 vibrational modes are possible [14]. According to group theory the optical phonon distribution is [15]

$$T= A_{1g}(R)+E_g(R)+T_{1g}+3T_{2g}(R)+2A_{2u}+2E_u+5T_{1u}(IR)+2T_{2u}$$

Where R and IR are Raman and Infrared activity modes respectively, $5T_{1u}$modes are infrared active mode, other five ($A_{1g}+E_g+T_{1g}+3T_{2g}$) modes are Raman active modes. These modes are composed to the motion of O ions and both tetrahedral and octahedral site ions [16-17]. The room temperature Raman data of $Ni_{0.5}Zn_{0.5}Fe_2O_4$ferrite sintered at 800ºC, 900ºC, 1000ºC, 1100ºC, and 1200ºC were carried in the frequency range 200 cm^{-1} to 1000 cm^{-1}.

Figure 2 shows the Raman spectra of the sintered samples indicating the characteristic peaks at 221, 246, 355, 452 with shoulder at 650 cm^{-1}. The Raman mode at 650 cm^{-1} was more promising at 1200^0C sintering temperature as it is increasing from 800^0C. This indicates the formation of mixed spinel ferrite is prominent at 1200^0C temperature.

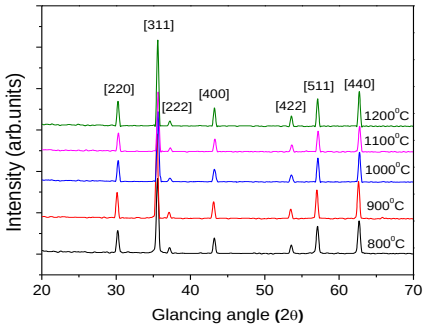

FIGURE 1. X-Ray Diffractograms of $Ni_{0.5}Zn_{0.5}Fe_2O_4$ sintered at 800^0C, 900^0C, 1000^0C, 1100^0C, and 1200^0C.

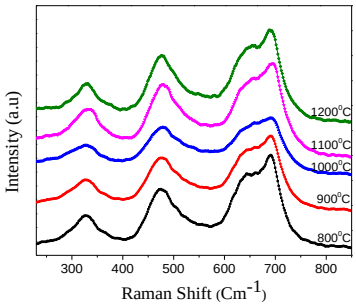

FIGURE 2. Raman spectra of $Ni_{0.5}Zn_{0.5}Fe_2O_4$ ferrite sintered at 800ºC, 900ºC, 1000ºC, 1100ºC, and 1200ºC with excitation wavelength of 532 nm.

Study of Micro structure is very important to understand the electrical properties of polycrystalline ferrites. The scanning electron microscopic (SEM) images of $Ni_{0.5}Zn_{0.5}Fe_2O_4$ ferrite sintered at different sintering temperatures was shown in figure 3. From SEM images it is very clear that grain size is increased with increasing of sintering temperature. The grain size is reported in the table 1. From SEM images it was observed that sintered samples contain grooves, pores, layers, cracks and sheet like patterns having some small aggregations within the available resolution. The observed sheet like structures gradually decreases to increasing of sintering temperature which leads to increase in grain size with increasing of sintering temperature. The grain size of all sintered samples measured by linear intercept method [18] and it was found to be linearly increases with increasing of sintering temperature and the obtained values in the range of 100nm-500nm. The obtained grain size values are very smaller than those reported in conventionally synthesized ferrites [19]. The observed smaller grain size values of sintered pellets can be explained on the basis of open and closed pores in the microstructure. Open pores are more effective at pinning than closed pores to restrict the growth of grain [20].

Table 1. Variation of Density, Crystallite size, Lattice Parameter, Grain Size, Relaxation time, Grain resistance, Grain capacitance of $Ni_{0.5}Zn_{0.5}Fe_2O_4$ ferrite samples with sintering temperatures.

Sintering temperature (^{0}C)	Density (gm/cm^3)	Crystallite size (nm)	Lattice parameter (Å)	Grain size (nm)	Relaxation time (τ) msec	Grain resistance (R_g) KΩ	Grain Capacitance (C_g) nf
800	3.35	32	8.391	117	43.6	22500	1.93
900	3.41	34	8.393	162	43.6	16800	2.6
1000	3.7	35	8.392	207	18.9	3240	5.82
1100	3.82	37	8.392	321	7.56	327	23.1
1200	4.01	39	8.394	508	2.81	47.7	58.8

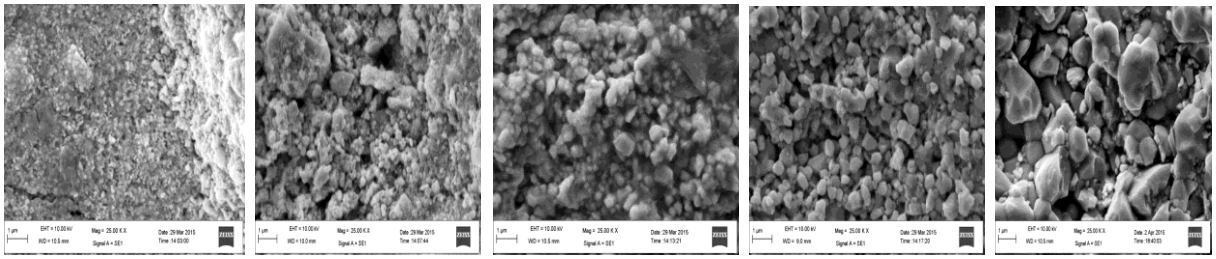

(a) (b) (c) (d) (e)

FIGURE 3.(a-e) SEM images of $Ni_{0.5}Zn_{0.5}Fe_2O_4$ sintered at (a) 800ºC, (b) 900ºC, (c) 1000ºC, (d) 1100ºC, and (e) 1200ºC.

Complex impedance spectroscopy is very important tool to understand the electrical properties of poly crystalline spinel type materials [21]. This is used to find grain, grain boundary resistance and relaxation time etc. In general polycrystalline ferrites have contributions from grain and grain boundary effects with two semi circles and high frequency side corresponding to grain resistance. Low frequency region belong grain boundary resistance. The complex impedance spectra of poly crystalline ferrites can be calculated by using the standard relation [21].

$$Z^* = Z' + iZ'' = \frac{R}{(1+i\omega\tau)}$$

$$Z' = \frac{R}{1+(\omega RC)^2} \text{ and } Z'' = \frac{\omega R^2 C}{1+(\omega RC)^2}$$

Where Z' is real part of impedance, Z'' is imaginary part of impedance, ω is angular frequency, and τ is relaxation time (τ=RC). The variation of frequency (log f) with real part of impedance (Z') indicates that the magnitude of Z' decreases that increasing frequency and sintering temperature were shown in figure 4(a). The Z' values merge to high frequency region due to release of space charge with rise of sintering temperature [22] this may be due to change in a.c conductivity in high frequency region. The variation of frequency with imaginary part of impedance Z'' is shown in figure 4(b). The curves in graph exhibit relaxation frequency f_{max}. These curves are shifted towards high frequency region with increase of frequency and sintering temperature. This indicates that the decrease of relaxation time τ. Then the domination space charge polarization occurred [23]. The room temperature Cole-Cole plots of Z' and Z'' was shown in figure 4(c). The impedance behavior of the samples is explained by using an equivalent circuit as shown in figure 4(d). From figure 4(a) single semicircular arc was observed in high frequency region which is corresponds to grain contribution $C_g = 1/R_g\omega_g$ where C_g and R_g capacitance and resistance of the grain. The values of C_g and R_g are reported in table 1. The relaxation time and grain resistance were decreased with increasing of sintering temperature.

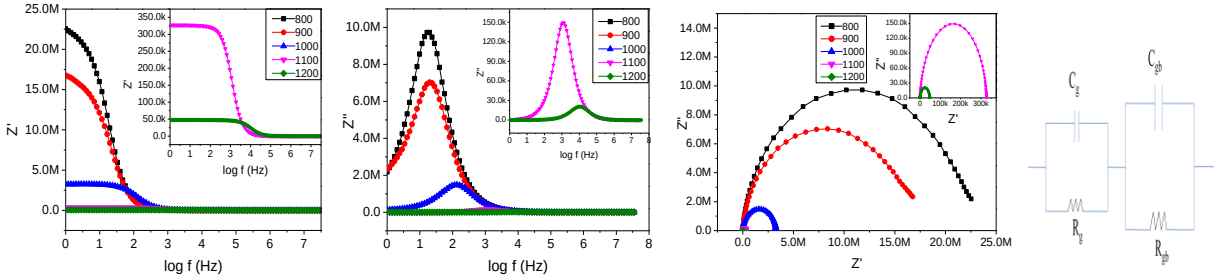

FIGURE 4.(a-d) Frequency variation real (a), imaginary (b) part of impedance, (c) cole-cole plots of $Ni_{0.5}Zn_{0.5}Fe_2O_4$ sintered at different sintering temperatures and (d) equivalent circuit.

The complex electrical modulus study is introduced to understand the electrical relaxation in ionically and electrically conducting materials. It is an advantage to suppressing the electrode polarizing effects [24-25]. the complex electric modulus M^* is calculated by using the following standard relation

$$M^* = M' + M'' = j\omega C_0 Z^*$$

Where $M' = \omega C_0 Z''$ and $M'' = \omega C_0 Z'$ are the real and imaginary parts of the complex electrical modulus respectively and C_0 is the geometrical capacitance $C_0 = \varepsilon_0 A/t$ (here A is the surface area of pellet, ε_0 is permittivity of free space and t is thickness of the sample). Figure 5(a) and 5(b) shows that the real and imaginary part of complex modulus spectra of $Ni_{0.5}Zn_{0.5}Fe_2O_4$ferrite sintered at 800^0C, 900^0C, 1000^0C, 1100^0C, and 1200^0C temperatures. From figure 5(a) the variation of real part of complex modulus with frequency at room temperature. Low frequency side the M' have very low value and it is increased with increasing of frequency and also it saturate at high frequency region. The dispersion is shifted to high frequency side with increasing of sintering temperature. From figure 5(b) the variation of imaginary part of complex modulus with frequency at room temperature from figure which is clearly observed that M'' have maximum value in low frequency side and the peak frequency is shifted with increasing of frequency and sintering temperature. Which indicates that the transition from long range to short range mobility with increasing of frequency. From figures of Z'' and M'' indicates that non-Debye type relaxation of the sample.

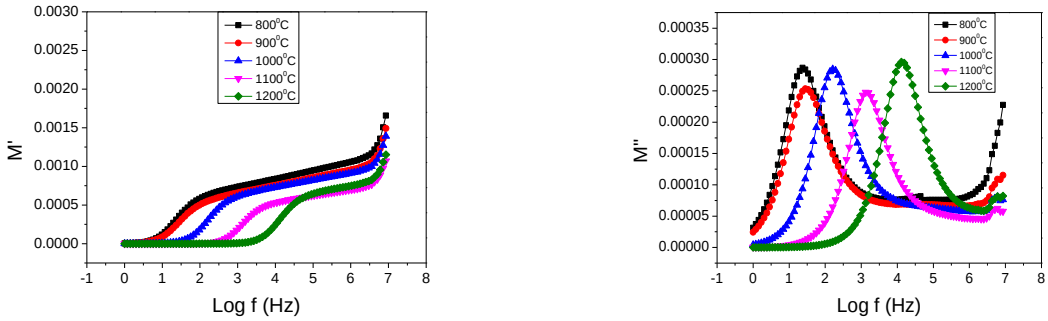

(a) (b)

FIGURE 5.(a-b) Variation of (a) real part and (b) imaginary part of complex electrical modulus with frequency at room temperature of $Ni_{0.5}Zn_{0.5}Fe_2O_4$ ferrite.

CONCLUSIONS

$Ni_{0.5}Zn_{0.5}Fe_2O_4$ is synthesized by citrate gel auto combustion method and sintered at various temperatures and conforms that the single phase spinel structure from XRD. Raman spectroscopy of all sintered samples indicated that are belongs to Fd3m space group. The grain resistance and grain capacitance were reported from impedance data indicating the non-Debye type relaxation nature of the sample.

ACKNOWLEDGMENTS

The authors are thankful to University Grants Commission, India, for providing financial assistance through UGC Major Research Project F.No.42-824/2013 (SR) Dt.22-03-2013.

REFERENCES

1. K. Kulikowski, J. Magn. Magn. Mater. **41** 56-62 (1984).
2. H. Igarash and K. Okazaki, J. Am. Ceram. Soc. **60** 51-54 (1977).
3. T. Abraham, Am. Ceram. Soc. Bull. **73** 62 (1994).
4. J. H. Liu, L. Wang and F. S. Li, J. Mater. Sci. **40** 2573 (2005).
5. H. Yang, X. C. Zhang, C. H. Huang, W. G. Yang and G. Z. Qiu, J. Phys. Chem. Solids **65** 1329 (2004).
6. P. K. Roy and J. Bera, J. Mater. Process. Technol. **197** 279-283 (2008).
7. S. Bid and S. K. Pradhan, Mater. Chem. Phys. **82** 27 (2003).
8. Tania jahanbin, Mansor hashim and Khamiral amin mantori J. Magn. Magn. Mater. **322** 2684-2689(2010).
9. Chandan Upadhyay, Devabrata Mishra, H. C. Verma, S. Anand and R. P. Das, J. Magn. Magn. Mater. **260** 188-194 (2003).
10. D. Chen, R. He, Mater. Res. Bull. **36** 13690-1377(2001).
11. Davuluri. Venkatesh, G. Himavathi and K. V. Ramesh, J Supercond Nov Magn. **28** 2801-2807 (2015).
12. A. C. F. M. Costa, E. Tortella, M. R. Morelli and R. H. G. A. Kiminami J. Magn. Magn. Mater. **256** 174 – 182 (2003).
13. D. Venkatesh, M. S. R. Prasad, B. R. Babu, K. V. Ramesh, and K. Trinath, Journal of Magnetics **20(3)**, 229-240 (2015).
14. W. B. White and B. A. Deangelis, Spectrochim. Acta A **23** 985 (1957).
15. Z. W. Wang, D. Schiferi, Y. S. Zhao and H. St. C. O'Neilr, J. Phys. Chem. Solids **64** 2517 (2003).
16. R. Gupta, A. K. Sood, P. Metcalf and J. M. Honig, Phys. Rev. B **65** 104430 (2002).
17. L. V. Gasparov, D. B. Tanner, D. B. Romero, H. Berger and G. Margaritondo, Phys. Rev. B **62** 7939 (2000).
18. J. C. Wurst and J. A. Nelson, J. Am. Ceram. Soc. **55** 109 (1972).
19. Su-il Pyun and Jong-tae Back, Am. Ceram. Soc. Bull. **64** 602(1985).
20. Cp. Camero and R. Raj, J. Am. Ceram. Soc. **71** 103 (1988).

21. E. Barsoukov and J. R. Macdonald, *Impedance Spectroscopy—Theory, Experiment and Applications* (Wiley, New Jersey, 2005).
22. B. Ramesh, S. Ramesh, R. Vijay Kumar and M. LakshmipathiRao, J. Alloys Compd. **513** 289 (2012).
23. R. V. Mangalaraja, S. Ananthakumar, P. Manohar and F. D. Gnanam, J. Magn. Magn. Mater. **253** 56 (2002).
24. A. Dias and R. L. Moreira, Mater. Lett. **39** 69 (1999).
25. N. Ponpandian and A. Narayanasamy, J. Appl. Phys. **92** 2770 (2002).